Ion Acceleration by Beating Electrostatic Waves: Domain of Allowed Acceleration

R. Spektor* **and E.Y. Choueiri†**
Electric Propulsion and Plasma Dynamics Laboratory (EPPDyL)
Mechanical and Aerospace Engineering Department
Princeton University, Princeton, New Jersey 08544

IEPC-01-209‡
October 14-19, 2001

The conditions under which an ion can be significantly accelerated through a nonlinear interaction with a pair of beating off-resonance electrostatic waves are explored. They are shown to differ substantially from the well-known criteria conditioning nonlinear ion acceleration by a single wave, which require that the initial ion velocity be above a certain threshold. The promise of this acceleration mechanism for propulsion applications stems from its capability of energizing ions from arbitrarily low initial velocity. A numerical investigation led to the identification of critical points on the reduced phase diagram whose positions characterize the motion. A second-order perturbation analysis of the location of these critical points was carried out to derive the criterion defining the allowed acceleration domain. It is shown that for an ion to be significantly energized, its initial total energy (Hamiltonian) must be above a critical value corresponding to the value of the Hamiltonian at the hyperbolic critical point. The resulting domain of allowed acceleration is significantly larger than that of ion acceleration by non-beating waves.

I. INTRODUCTION

Stochastic heating of a magnetized ion in presence of a single obliquely as well as perpendicularly propagating electrostatic (ES) wave has been extensively studied [1–4]. Using first-order perturbation theory Karney [5] was able to derive analytical expressions approximating overall dynamics of ions interacting with such a wave. Skiff *et al.* validated these findings experimentally [6]. Another important result shown by Karney was the existence of an ion energy threshold below which the particle cannot gain energy from the ES wave. This threshold is essentially the lower bound of a nonlinearly broadened resonance condition between the ion thermal and wave phase velocities. Also this threshold was found to separate two regions of the phase space: a *regular* (or coherent) motion region of low energies below the threshold and a *stochastic* one - above the threshold. Nonlinear ion acceleration (or energization) by a single wave is therefore always a stochastic process.

In 1998 Benisti *et al.* suggested a radically new scheme for nonlinear ion acceleration by ES waves [7, 8]. The scheme requires *pairs* of ES waves such that their corresponding frequencies differ by an integer number of the cyclotron frequency of the gyrating ion. In essence these waves create a beating wave that interacts with the ion. Under such conditions the single-wave theory threshold disappears and regular and stochastic regions become connected allowing ions with arbitrary small initial velocities to obtain high energies through coherent acceleration followed by stochastic energization. Consequently, this nonlinear interaction may result in a more efficient acceleration mechanism than is possible from the ion's interaction with a single wave. This new acceleration scheme has been advanced as a possible explanation for the ionospheric ion acceleration observed during the Topaz 3 rocket [9] experiments.

An acceleration mechanism that promises to energize a larger portion of the ion distribution function may be promising to many applications where the efficiency of ion acceleration is of prime importance, such as in plasma propulsion applications.

In this paper we study the nonlinear interaction between a magnetized ion and a pair of beating waves by considering a large number of ion trajec-

---

*Graduate Student, Research Assistant.
†Chief Scientist at EPPDyL.
‡Presented at the 27^{th} International Electric Propulsion Conference (IEPC), Pasadena, California

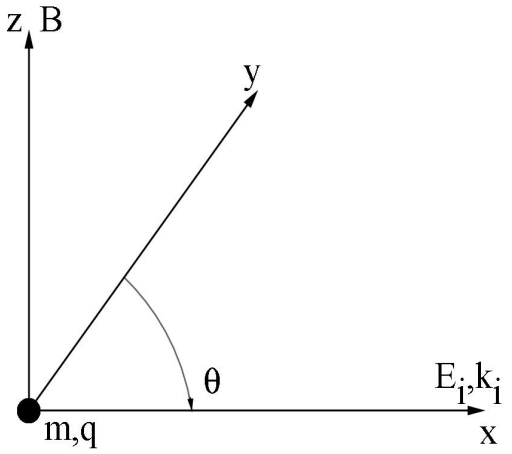

FIG. 1: A single ion of charge q and mass m in a constant homogeneous magnetic field $\mathrm{B}\hat{z}$ interacts with a spectrum of electrostatic waves whose wavenumber and electric field direction is parallel to the x-axis.

tories (each representing a different initial condition) in the generalized phase space (Poincaré cross-section) instead of only looking at a single ion trajectory as was done in Refs. [7, 8] and our previous work [10]. This approach allows us to improve our understanding of ion dynamics by finding the critical points[11] of the motion, as well as to define particle's dynamics in terms of the location of these critical points. With that in mind, we use second-order perturbation theory and combine analytical and numerical solutions to investigate the nature of ion motion for a wide range of parameters involved. Specifically we focus on finding the criteria for the transition to stochastic acceleration which amounts to a definition of the domains of allowed and forbidden acceleration.

In section II we overview the analytical formulation of the problem. Then in section III we summarize the better-known results of the single wave case. We introduce multiple wave interaction in section IV. In section IV A we explain the ion dynamics in such an interaction when no beating wave is created and in section IV B we contrast that with the case of a beating pair of waves and derive the governing criterion defining the allowed acceleration domain.

II. ANALYTICAL FORMULATION

We first proceed to mathematically define the problem. Fig. 1 shows the coordinate system setup. Here we have a single ion of mass m and charge q in a constant and homogeneous magnetic field, $\mathrm{B}\hat{z}$. This ion interacts with a spectrum of electrostatic waves that propagate in the positive x direction. The wave number k_i as well as the electric field direction of each of these waves is parallel to the x-axis. The motion of the single ion in Fig. 1 is described by the following equation of motion, [7]

$$\frac{d^2x}{dt^2} + \omega_c^2 x = \frac{q}{m}\sum_i E_i \sin(\mathrm{k}_i x - \omega_i t + \varphi_i), \quad (1)$$

where $\omega_c = q\mathrm{B}/m$ is the ion cyclotron frequency, k is the wavenumber, and φ_i is the phase angle of each wave. The corresponding Hamiltonian for the system is [7]

$$\bar{H} = \rho^2/2 + \sum_i \frac{\varepsilon_i}{\kappa_i}\cos(\kappa_i \rho \sin\theta - \nu_i \tau + \varphi_i). \quad (2)$$

In writing Eq. (2) we have used the fact that the system is periodic, and transformed the Hamiltonian into normalized action-angle coordinate system [12] where $\kappa_i = \mathrm{k}_i/\mathrm{k}_1$, $\nu_i = \omega_i/\omega_c$, $\tau = \omega_c t$, $\varepsilon_i = (\mathrm{k}_1 q E_i)/(m\omega_c^2)$, $\rho^2 = X^2 + \dot{X}^2$, and $X = \mathrm{k}_1 x$, $\dot{X} = dX/d\tau$, so that $X = \rho\sin\theta$, $\dot{X} = \rho\cos\theta$. The action-angle coordinate system is a special case of polar coordinates[11]. In our context θ corresponds to the cyclotron phase angle measured clockwise from the y-axis, as indicated on Fig. 1, while ρ is the normalized Lamor radius which, in a constant magnetic field, represents the normalized velocity (perpendicular to the magnetic field) of the magnetized particle undergoing cyclotron motion in the xy plane.

Benisti *et al.* [7] defined a criterion for particle acceleration by multiple ES waves. They showed that for regular and stochastic regions to be connected it is necessary (but, as we shall see, not sufficient) to have at least one pair of ES waves such that

$$\omega_2 - \omega_1 = n\omega_c, \quad (3)$$

where n is an integer. Consequently, for the sake of simplicity, we reduce our analysis to the case of a single pair of beating waves. In addition, Ref.[7] reports that the maximum acceleration is achieved when all waves are of the same amplitude. Therefore we set $\varepsilon_i = \varepsilon_j = \varepsilon$ and $\kappa_i = \kappa_j = 1$. As stated in Ref.[7], the phase angles, φ_i, do not play a fundamental role in the acceleration process so we set all $\varphi_i = 0$. With these simplifications the Hamiltonian (2) becomes

$$\bar{H} = \rho^2/2 + \varepsilon[\cos(\rho\sin\theta - \nu_i\tau) + \cos(\rho\sin\theta - \nu_j\tau)]. \quad (4)$$

Adopting the criterion described by Benisti *et al.* for the two wave frequencies, we note that the Hamiltonian (4) could be viewed either as a time-dependent system with one degree of freedom or as an autonomous system with two degrees of freedom, since the system is periodic [12]. We adopt the latter approach. In this view the Hamiltonian represents two coupled oscillators: one is the gyrating ion and the other corresponds to the ES waves. When the frequency ratio of these two oscillators equals p/q, where p and q are relatively prime integers, the system is said to be *in resonance* [5, 11].

Two approaches are taken in this paper for analyzing the system above. Eq. (4) is integrated numerically and the solutions are then compared to the analytical solutions derived by applying a second-order perturbation technique in conjunction with Lie transformations [11].

A convenient way of representing both numerical and analytical solutions is by plotting the resulting trajectories on a Poincaré cross-section (which is a reduced phase space diagram). In this paper Poincaré cross-sections are plots in the ρ-θ plane at $(\nu\tau)_{mod\,2\pi}$. Since the magnetic field is constant ρ, the normalized cyclotron radius, is a direct measure of the perpendicular ion velocity. Therefore Poincaré cross-sections give direct visual insight into the acceleration process.

To construct a Poincaé cross-section we plot the point intersections of the ion trajectory in three dimensions (ρ, θ, τ) with the ρ-θ plane. Random point distribution on the Poincaré cross-section correspond to stochastic motion while regular patterns, such as lines and ellipses, will tell us that the ion dynamics is regular (sometimes called coherent). For example, if the wave amplitude, ε, is zero, Eq. (4) reduces to a simple harmonic oscillator and for irrational ν its Poincaré cross-section shows a set of horizontal lines, indicating constant velocity (which corresponds to a free ion gyrating in a constant magnetic field.) Each of these lines represents an invariant of motion for a given set of initial conditions [11]. When ε is not zero we can treat the ion motion as a perturbation of these invariants.

The detailed derivation of the analytical solution of a single wave-particle interaction could be found in Ref.[5]. However, a more generalized solution for multiple waves is obtained [7, 13, 14] through Deprit's modified Lie transformation in Ref. [11]. The resulting autonomous Hamiltonian derived from Eq. (4) for ν = integer to the second order in the perturbation, ε, is

$$\begin{aligned} H &= \varepsilon\{J_{\nu_i}(\rho)\cos(\nu_i\theta) + J_{\nu_j}(\rho)\cos(\nu_j\theta)\} \\ &+ \varepsilon^2\{S_1^{\nu_i}(\rho) + S_1^{\nu_j}(\rho) \\ &+ S_6^{\nu_i,\nu_j}(\rho)\cos[(\nu_j - \nu_i)\theta]\}, \end{aligned} \tag{5}$$

where,

$$\begin{aligned} S_1^{\nu_i}(\rho) &= \frac{1}{2\rho}\sum_{m=-\infty}^{\infty}\frac{mJ_m(\rho)J'_m(\rho)}{\nu_i - m}, \\ S_6^{\nu_i,\nu_j}(\rho) &= \frac{1}{2\rho}\Bigg(\sum_{m=-\infty}^{\infty}\frac{mJ_m(\rho)J'_{\nu_j-\nu_i+m}(\rho)}{\nu_i - m} + \\ &+ \sum_{m=-\infty}^{\infty}\frac{mJ_m(\rho)J'_{\nu_i-\nu_j+m}(\rho)}{\nu_j - m}\Bigg). \end{aligned} \tag{6}$$

and where J_m is the Bessel function of the first kind of order m, and J' represents the derivative of the Bessel function with respect to its argument. When ν_i is an integer, the summations are performed over all $m \neq \nu_i$ to avoid singularities. When $\nu \neq$integer, the first order terms in Eq. (5) disappear [7].

The Hamiltonian in Eq. (5) is autonomous and therefore itself is an invariant of motion. By plotting curves of constant H we obtain a Poincaré cross-section which gives us the complete analytical solution of the problem to the second order.

We wish to compare the Poincaré cross-sections of the analytical solution to those obtained through numerical integration of Eq. (4). To obtain the numerical solution we have developed a code based on the fourth order symplectic integration algorithm derived by Candy and Rozmus [15] who showed its superiority over Runge-Kutta algorithm for Hamiltonian periodic problems.

As with most phase diagrams, critical (or fixed) points define the dynamics of motion. Since the system is not dissipative we expect to find two types of critical points: elliptic and hyperbolic. Moreover, these critical points represent the nonlinear resonances described above. As we will show later, critical points play the key role in determining whether ion motion is regular or stochastic. The task before us is to find these critical points.

That task can be achieved by setting the time derivative of ρ and θ to zero simultaneously [11, 16].

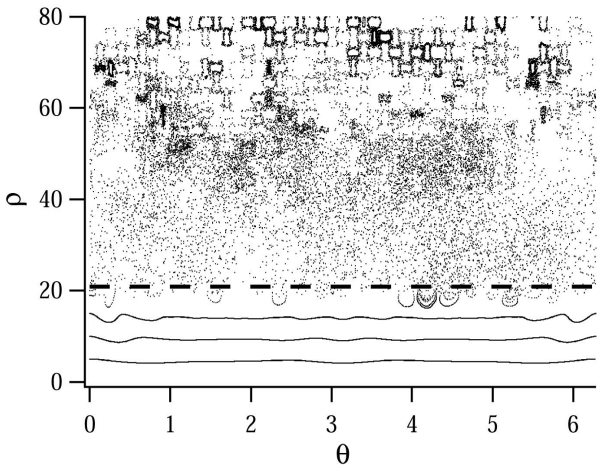

FIG. 2: Poincaré cross-section showing numerical solutions for a particle interacting with a single *on-resonance* wave ($\varepsilon = 10$, $\nu = 24$). The threshold derived in Ref.[5] and given by Eq. 9 represents the boundary between the regular and stochastic domains and is shown as a horizontal thick dashed line.

Utilizing Hamilton's equations of motion we get

$$\begin{aligned}\dot{\rho} &= \frac{\partial H}{\partial \theta} = \varepsilon\{\nu_i J_{\nu_i}(\rho)\sin(\nu_i\theta) \\ &+ \nu_j J_{\nu_j}(\rho)\sin(\nu_j\theta)\} \\ &+ \varepsilon^2(\nu_i-\nu_j)S_6^{\nu_i,\nu_j}(\rho)\sin[(\nu_j-\nu_i)\theta] = 0, \end{aligned} \tag{7}$$

$$\begin{aligned}\dot{\theta} &= -\frac{\partial H}{\partial \rho} = \varepsilon\{J'_{\nu_i}(\rho)\cos(\nu_j\theta) \\ &+ J'_{\nu_j}(\rho)\cos(\nu_j\theta)\} \\ &+ \varepsilon^2\{S_1^{'\nu_i}(\rho) + S_1^{'\nu_j}(\rho) \\ &+ S_6^{'\nu_i,\nu_j}(\rho)\cos[(\nu_i-\nu_j)\theta]\} = 0. \end{aligned} \tag{8}$$

When both wave frequencies are *off-resonance* ($\nu_i, \nu_j \neq integer$), the equations above simplify because the first order terms drop out, and we are able to obtain the position of critical points analytically.

We now explore particle dynamics as a function of wave amplitude and frequency, and in terms of the location of critical points on the Poincaré cross-section. Using numerical solutions we will demonstrate that when critical points are absent in the regular region of the Poincaré cross-section (as in the single wave-particle interaction), the particle will not gain energy.

III. SINGLE WAVE INTERACTION

In this section, in order to create a context for our study, we summarize the results obtained by Kanrey [5] for the interaction of a magnetized particle with a single wave. When the wave frequency is exactly an integer number of the ion cyclotron frequency it is said to be an *on-resonance* wave, otherwise it is an *off-resonance* wave. In both cases Karney found that a threshold value of ρ, given by

$$\rho = \nu - \sqrt{\varepsilon}, \tag{9}$$

separates the regions of regular and stochastic motion [5, 17], as shown Fig. 2. Below the threshold, indicated by the horizontal thick dashed line, we observe smooth lines representing the invariants of motion. This is where the ion motion is regular and we can predict its behavior well by means of perturbation theory. However, as long as the ion's initial velocity, ρ_0, is in that region it is clear that the ion will not gain much energy from the wave. Therefore, in the case of interaction with a single wave the ion gains energy only chaotically when its initial velocity ρ_0 exceeds the threshold, i.e.

$$\rho_0 > \nu - \sqrt{\varepsilon}. \tag{10}$$

This is an important point and will be contrasted later with the case of beating waves where, as we shall see, the two regions of the phase space become connected and a particle with an arbitrarily small initial velocity in the regular region can be accelerated through the threshold to high values of ρ. Motion in the stochastic region of phase space can be approximated by perturbation solutions when the wave amplitude (perturbation strength), ε, is small enough [5, 7].

IV. MULTIPLE WAVE INTERACTION

One of the early investigations of two ES waves interacting with ions was done by Chia *et al.* [13] (1996) who conducted an analytical study of the interaction to the first order in the perturbation and came close to discovering the new acceleration mechanism by noting that, for the waves with even-even or odd-odd combinations of frequencies (ν), there existed a radial separatrix allowing "infinite" heating. In 1998 Benisti *et al.* [7, 8] showed that to observe particle acceleration through the threshold boundary one needs to use perturbation theory to at least *second* order. Then, the condition for the new acceleration mechanism already given by Eq. (3) is

$$\nu_j - \nu_i = n. \tag{11}$$

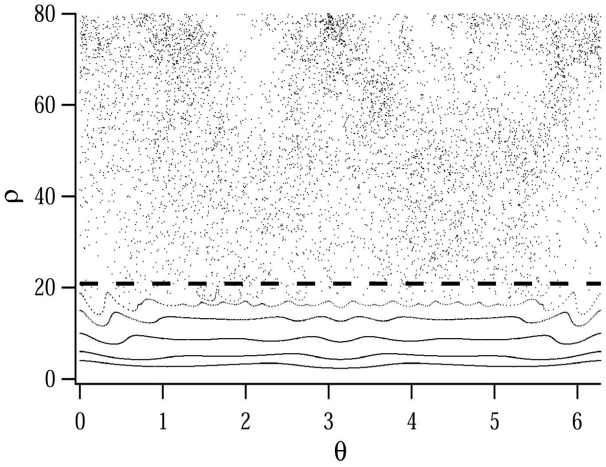

FIG. 3: Poincaré cross-section showing numerical solutions for a particle interacting with two non-beating waves ($\varepsilon = 10$, $\nu_i = 24$, $\nu_j = 25.5$). Particles with initial velocity below the threshold defined by Eq. (9), shown as a dashed line, are seen not gain energy from the waves. This picture is qualitatively similar to that in Fig. 2.

where n is an integer. This amounts to a wave beating condition.

A. Non-Beating Waves

We start with the case of a particle interacting with multiple waves, when Eq. (11) does not hold. Fig. 3 shows a typical Poincaré cross-section obtained with numerical solutions for $\varepsilon = 10$, $\nu_i = 24$, and $\nu_j = 25.5$. The picture is qualitatively very similar to that of the single wave-particle interaction shown in Fig. 2. Ions with energies below some threshold do not gain much energy. Extrapolating from a single particle picture to the case of a plasma with a velocity distribution one expects that particles lying below the threshold will remain unaffected. This picture changes qualitatively if condition (11) is satisfied.

B. Beating Waves (Off-Resonance)

As we already mentioned above, in the case of the *off-resonance* beating waves (both ν_1 and ν_2 are not integers) we can make approximations that greatly simplify our analysis. Consequently, we will focus our attention on such cases. Some qualitative analysis of the *on-resonance* beating waves is still possible and will be done in the next section.

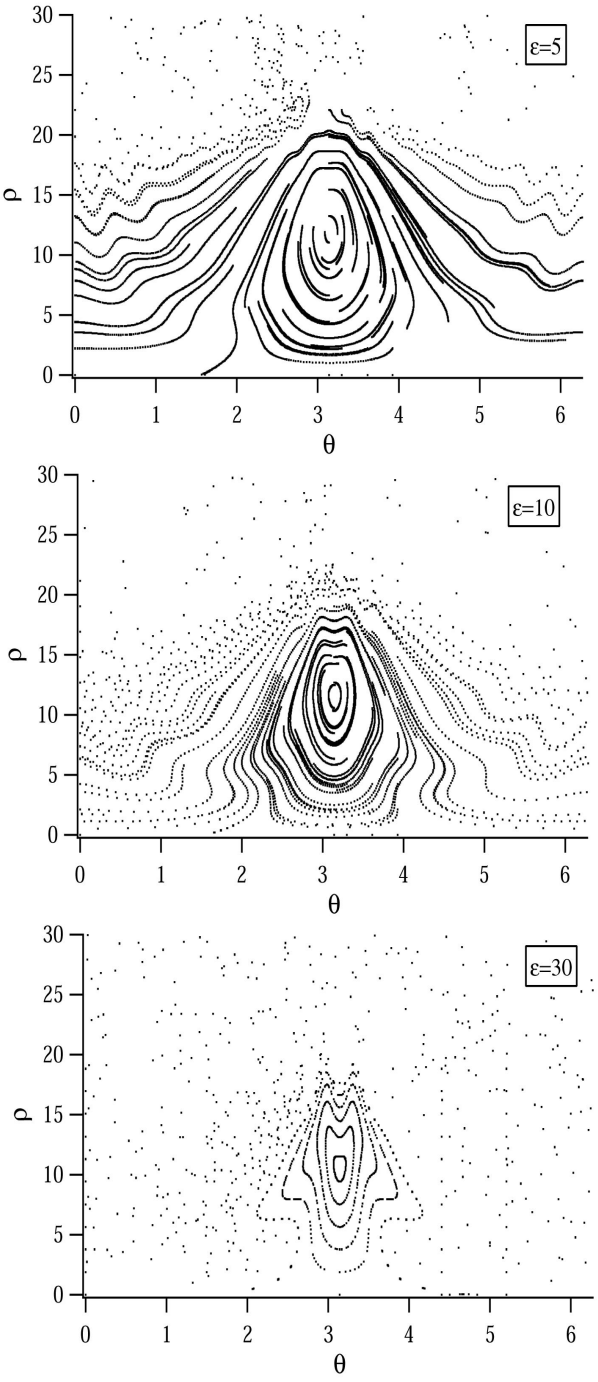

FIG. 4: Poincaré cross-sections showing numerical solutions for a particle interacting with two beating off-resonance waves ($\nu_i = 24.3$, $\nu_j = 25.3$). The stochastic region occupies a greater fraction of the phase space as the wave amplitude is increased.

We show typical Poincaré cross-sections for different values of ε in Fig. 4 where numerical solutions for $\nu_i = 24.3$ and $\nu_j = 25.3$ illustrate the effect of increasing wave amplitude. The phase diagram consists of two regions, stochastic and regular, just as for the single wave interaction, with the important feature that the two regions are "connected". An ion with low initial velocities can undergo first regular and then stochastic acceleration, reaching high energies. We explored this behavior and its dependence on the wave energy in Ref. [10] using a single trajectory.

At low perturbation (low values of ε) the regular region extends to values of ρ approximately predicted by Eq. (9). However, as ε is increased the regular region quickly shrinks to the vicinity of the elliptic critical point (designated E on Fig. 5.) Eventually, as the wave amplitude is raised above values shown on Fig. 4, chaotic motion dominates the phase diagram.

Eq. (4) can be rewritten as

$$\bar{H} = \frac{\rho^2}{2} + \varepsilon \cos(\frac{n}{2}\tau) \cos[\rho \sin\theta - (2\nu_i + n)\tau]. \quad (12)$$

The argument of the first cosine term tells us that the frequency of the beating wave is half an integer times the ion cyclotron frequency (ω_c). It is not surprising perhaps that we will later find a critical point corresponding to the resonance between the ion's gyro motion and the waves at $\rho \simeq \nu/2$, as can be gleaned from Fig. 5. We defer the discussion of critical points to section IV B 2. For simplicity we will now limit our discussion to $n = 1$.

Let's now gauge how well the second-order perturbation analysis compares to the numerical solutions. Fig. 5 indicates a good degree of agreement between the two. Even though the detailed structure of the regular motion lines is not captured with the analytical solution, the latter does predict the position of the lower elliptic (E) as well as that of the hyperbolic point (H) rather well. In the analytical solutions shown in Fig. 5 we observe more critical points at $\rho > 20$. These don't appear in the numerical solution, instead they are covered by points representing stochastic motion. However, as shown in Ref.[8], even in that region of phase space the overall ion motion could be approximated by first-order orbits, for small ε.

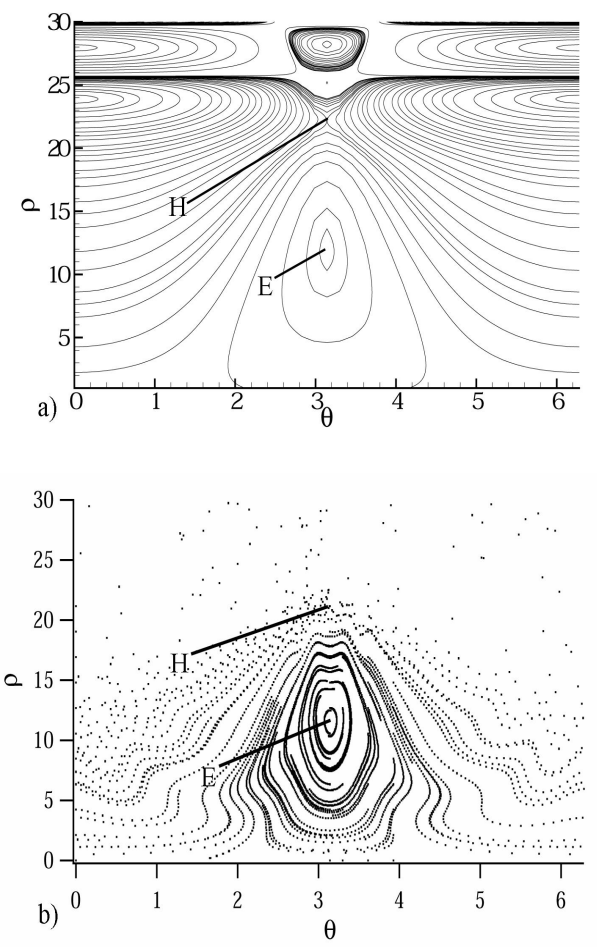

FIG. 5: Poincaré cross-section for a particle interacting with two beating off-resonance waves ($\varepsilon = 10$, $\nu_i = 24.3$, $\nu_j = 25.3$). a) Analytical solution showing the existence of hyperbolic and elliptic points marked by H and E respectively. b) Numerical solution also showing the locations of the critical points.

1. *Topology of the Phase Diagram*

As with any phase diagram, each line on the Poincaré cross-section corresponds to a given set of initial conditions. In the case of a particle interacting with beating waves we are mainly concerned with the hyperbolic and an the elliptic critical points designated H and E on Fig. 5. These points can indicate whether or not the ion will gain net energy from the waves. It is clear by tracing trajectories in Figs. 4 and 5 that an ion with an initial energy (Hamiltonian value) lying between the Hamiltonian values corresponding to points E and H does not gain net energy from the waves i.e. reach the stochastic region where it can be vigorously accelerated. Instead the corresponding phase space trajectories venture around the elliptic critical point E. (It is relevant to note in this context that the Hamiltonians of various trajectories increase monotonically from the Hamil-

tonian value at point E to its value at point H.)

Therefore, for given values of ν_i and ϵ, the inequality

$$H(\rho_0;\theta_0) > H_H \tag{13}$$

defines the *allowed acceleration domain*. By "allowed acceleration domain" we mean here the domain of initial conditions for which an ion can reach the stochastic region of phase space where it can be vigorously energized.

The acceleration criterion in Eq. (13) should be contrasted with that for single-wave interaction given by Eq. (10). It is clear that unlike the single-wave case, an ion with initial **velocity** ρ_o below the threshold given by Eq. (10) can still be accelerated as long as its **Hamiltonian** is above a certain threshold (H_H).

From the point of view of plasma acceleration one would like to limit the number of particles trapped in the forbidden acceleration domain ($H_E < H < H_H$). The rest of the ions gain much higher energies through first regular (if their initial energy is low) then stochastic acceleration, as shown in Figs. 4 and 5.

It is interesting to note that point E lies exactly at $\theta = \pi$. That corresponds to the moment when the ion is moving in the negative x direction, against the waves (see Fig. 1). At this resonance point the energy exchange is minimum and the situation is equivalent to a ball bouncing between stationary walls at constant energy. In the immediate neighborhood of point E the ion energy cannot be altered sufficiently to push it into the stochastic region. From numerical analysis (Fig. 4) the value of ρ at point E can be estimated to be roughly half of the single wave threshold condition (9). This will be explored further analytically in the next section.

When we choose ν_i and ν_j to be both *on-resonance*, the overall behavior becomes much more complicated. Fig. 6 shows the case with $\varepsilon = 10$, $\nu_i = 24$, and $\nu_j = 25$. The major difference with respect to the *off-resonance* cases is that now we have two hyperbolic points which do not lie at $\theta = \pi$. Also, the analytical solution shows us much more complicated chains of the critical points at large ρ. This also indicates that the analytical treatment of the *on-resonance* cases is more difficult. Consequently we choose to study only *off-resonance* cases in the next section.

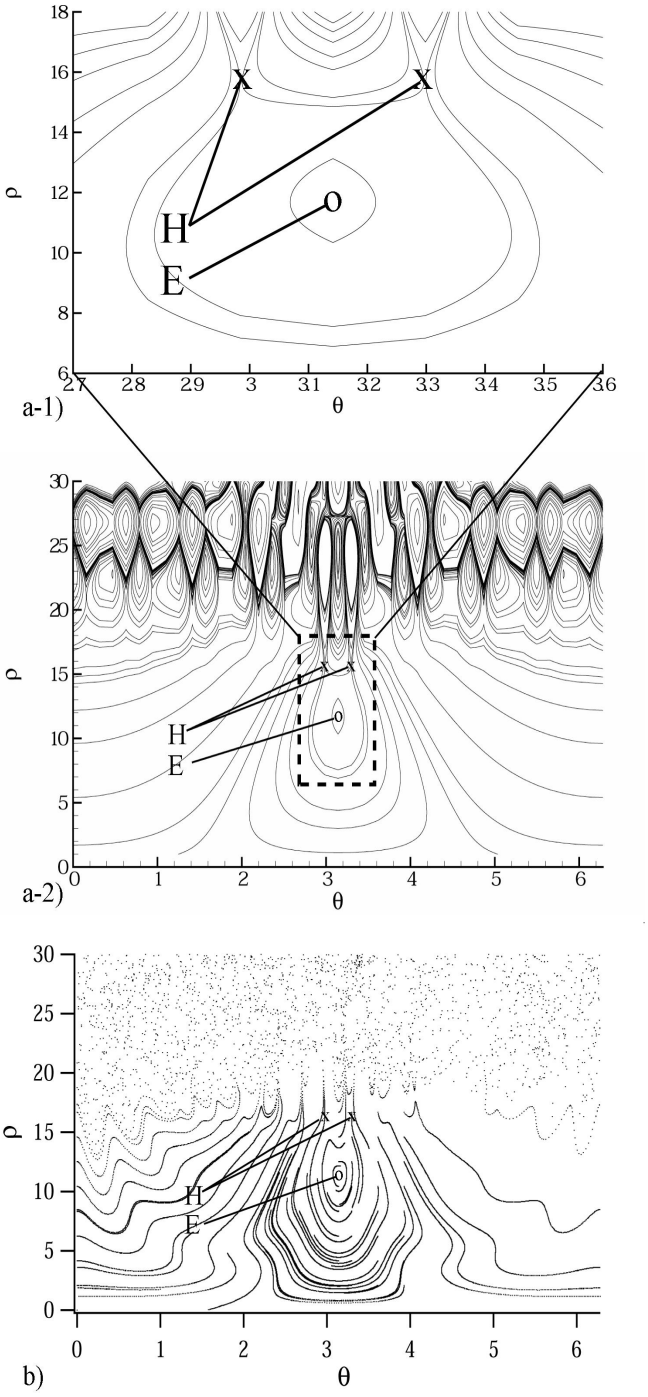

FIG. 6: Poincaré cross-section for a particle interacting with two beating on-resonance waves showing a more complicated picture than that of the off-resonance case shown in Fig. 5. ($\varepsilon = 10$, $\nu_i = 24$, $\nu_j = 25$). a.1 and a.2) analytical solution. b) numerical solution.

2. *Critical Points*

Defining the domain of allowed acceleration described by Eq. (13) therefore amounts to finding an

expression for the location of the critical point H. Knowing also the location of the elliptic point E gives additional insight into the problem. We now seek analytical expressions for both.

For $\nu \neq$ integer, the $S_1^{\nu_i}(\rho)$ term in Eq. (6) could be simplified to[13]:

$$S_1^{\nu_i}(\rho) = \frac{\pi}{8\sin\nu_i\pi}[J_{\nu_i+1}(\rho)J_{-(\nu_i+1)}(\rho) - J_{\nu_i-1}(\rho)J_{-(\nu_i-1)}(\rho)]. \quad (14)$$

Note that the above simplification does not hold when ν is an integer which is the case of the less-tractable *on-resonance* interaction. As shown in the appendix we can simplify the $S_6^{\nu_i,\nu_j}(\rho)$ term down to

$$S_6^{\nu_i,\nu_j}(\rho) = \frac{\rho}{\nu_i}S_1^{\nu_i}(\rho) + \frac{\rho}{\nu_j}S_1^{\nu_j}(\rho). \quad (15)$$

We can therefore express the Hamiltonian (5) in terms of the simplified $S_1^{\nu_i}(\rho)$ function only,

$$H = \varepsilon^2\Big\{(1+\frac{\rho}{\nu_i}\cos[\nu_i-\nu_j]\theta)S_1^{\nu_i}(\rho) + (1+\frac{\rho}{\nu_j}\cos[\nu_i-\nu_j]\theta)S_1^{\nu_j}(\rho)\Big\}. \quad (16)$$

Here we dropped the first-order terms as they were shown to be negligible by Benisti *et al.* [7, 8] in the region $\rho < \nu - \sqrt{\varepsilon}$. Taking $\rho/\nu_i \sim \rho/\nu_j$ and dropping the subscripts in $S_1^{\nu_i}(\rho)$ we have

$$H = \varepsilon^2\left[1+\frac{\rho}{\nu_i}\cos(\nu_i-\nu_j)\theta\right]\times \left[S^{\nu_i}(\rho)+S^{\nu_j}(\rho)\right]. \quad (17)$$

Finally, we substitute Eq. (14) for each of the $S_1^{\nu_i}(\rho)$ functions. Recalling Eq. (11) with $n=1$ and expressing everything in terms of ν_i we get

$$H = \frac{\varepsilon^2\pi}{8\sin\nu\pi}\left(1+\frac{\rho}{\nu}\cos\theta\right) \quad (18)$$
$$\Big[- J_{\nu-1}(\rho)J_{-(\nu-1)}(\rho) + J_\nu(\rho)J_{-\nu}(\rho) + J_{\nu+1}(\rho)J_{-(\nu+1)}(\rho) - J_{\nu+2}(\rho)J_{-(\nu+2)}(\rho)\Big],$$

where we have replaced ν_i with ν.

We now proceed to find the position of points E and H. From Figs. 4 and 5 we know that these points lie at $\theta = \pi$. This reduces equations (7) and (8) to

$$\frac{\partial}{\partial\rho}(1-\frac{\rho}{\nu})L(\rho) = 0, \quad \text{where,} \quad (19)$$
$$L(\rho) = -J_{\nu-1}(\rho)J_{-(\nu-1)}(\rho) + J_\nu(\rho)J_{-\nu}(\rho) + J_{\nu+1}(\rho)J_{-(\nu+1)}(\rho) - J_{\nu+2}(\rho)J_{-(\nu+2)}(\rho).$$

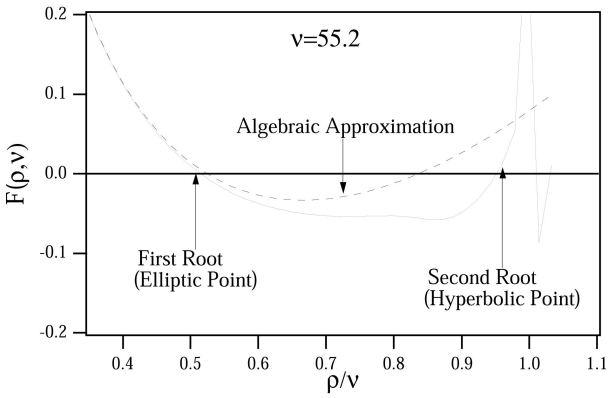

FIG. 7: Plot of the function $F(\rho,\nu)$, given by Eq. (20), showing the two roots corresponding to the two critical points. The algebraic approximation to $F(\rho,\nu)$, given by Eq. (21), is also shown as a dashed curve.

From Eq. (19) we can express ρ as a function of $L(\rho)$ and $L'(\rho)$, where the prime denotes the derivative with respect to ρ, and arrange the resulting expression as

$$F(\rho,\nu) \equiv \frac{\rho}{\nu} + \frac{L(\rho)}{\nu L'(\rho)} - 1 = 0, \quad (20)$$

whose the first and second roots, ρ_E and ρ_H, for a given value of ν, correspond to the locations (with $\theta=\pi$) of the elliptic and hyperbolic points respectively.

The expression in the above equation is plotted as a function of ρ/ν for $\nu = 55.2$ and shown as the hard curve in Fig 7. The first root, ρ_E, occurs near $\rho/\nu \simeq 0.5$ and the second root, ρ_H, occurs in the vicinity of $\rho/\nu \simeq 0.9$.

The location of the elliptic critical point can also be approximated by the root of the following algebraic expression which does not involve Bessel functions and which is obtained from Eq. (20) after some involved algebra using Bessel function recursive relations and associated continued fraction representations[18],

$$F(\rho,\nu) \simeq \frac{\rho}{\nu} - 1 + \frac{2}{3\left(f_{\nu-1}+f_{-(\nu-1)}+f_{\nu+2}+f_{-(\nu+2)}\right)} = 0 \quad (21)$$

where the function $f_\nu = f_\nu(\rho) \equiv J'_\nu/J_\nu$ is given by

$$f_\nu \simeq \frac{\rho}{\nu} - \frac{\frac{\nu}{\nu+1} - \frac{1}{4}\left(\frac{\rho}{\nu}\right)^2\left(\frac{\nu}{\nu+2}\right)^3}{\frac{2}{(\rho/\nu)} - \frac{\rho}{\nu}\left(\frac{\nu}{\nu+2}\right)^2}. \quad (22)$$

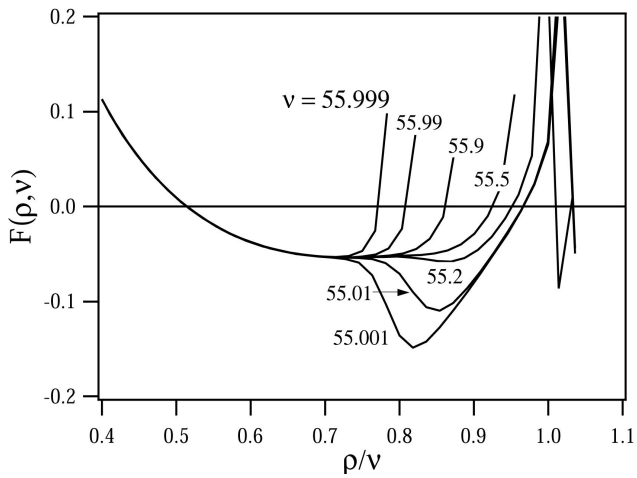

FIG. 8: Plot of the function $F(\rho, \nu)$, given by Eq. (20), showing how the second root (corresponding to the hyperbolic point) moves away from $\rho/\nu = 1$ as ν changes from 55.001 to 55.999.

The above approximation is valid for $\nu \gg 1$ and $\rho \geq \sqrt{\nu(\nu+1)}$ and is plotted as a dotted curve in Fig 7 for the case of $\nu = 55.2$.

We evaluated the location of the first root for a wide range of ν values and tabulated the results in the second column of Table I. It is seen that for $\nu \gg 1$ this first root can be expressed as $\rho/\nu \simeq 0.5$, therefore the location of the elliptic point, according to our second-order perturbation analysis, is at

$$\rho_E \simeq \frac{\nu}{2}. \tag{23}$$

The location of the hyperbolic critical point corresponds to the second root of Eq. (20) and is seen, in Fig 7, to be near the point at which the function becomes oscillatory due to the oscillatory behavior of the Bessel functions which is onset when the argument of the Bessel function reaches the "turning point" [18] $\rho_{tp} = \sqrt{\nu(\nu+1)}$. We can therefore **roughly** approximate the location of the hyperbolic point by

$$\rho_H \simeq \sqrt{\nu(\nu+1)} \simeq \nu, \tag{24}$$

where the last inequality holds when $\nu \gg 1$.

It is relevant to note that a numerical evaluation of the location of the second root of Eq. (20) over a wide range of ν values yielded values of ρ_H/ν that are less than unity as tabulated in the third column of Table I. Indeed, the plot in Fig 8 of the function in Eq. (20) for values of ν ranging from 55.001 and 55.999 shows that, while the location of the first root is largely independent of ν (for $\nu >> 1$), the location of the second root depends on the difference between ν and its nearest lower integer. Therefore a more accurate representation of the location of the hyperbolic point is

ν	ρ_E/ν	ρ_H/ν
9.7	0.48	0.65
12.1	0.49	0.88
24.3	0.52	0.9
33.8	0.52	0.84
43.9	0.52	0.84
55.2	0.51	0.95
62.4	0.51	0.94

TABLE I: Positions of the critical points, ρ_E and ρ_H, normalized by ν, corresponding to the roots of Eq. (20) for a range ν values.

$$\rho_H \simeq \psi\nu. \tag{25}$$

where ψ is generally a function of ν and the difference between ν and its nearest lower integer

$$\psi = \psi[\nu; (\nu - \perp\nu)] \simeq 1 \tag{26}$$

where $\perp\nu$ is the bottom (or floor) of ν and the semi-equality holds when $(\nu - \perp\nu) \ll 1$.

V. SUMMARY AND CONCLUDING REMARKS

A numerical investigation of the nonlinear acceleration of a magnetized ion by a pair of beating electrostatic waves led to the identification of critical points on the reduced phase diagram whose positions characterize the motion. A second-order perturbation analysis of the location of these critical points was carried out to derive the criterion defining the allowed acceleration domain.

For a pair of off-resonance ($\nu_1, \nu_2 \neq$ integer), beating ($\nu_1 - \nu_2 = 1$), electrostatic waves interacting nonlinearly with a magnetized ion, significant ion acceleration can occur when the Hamiltonian satisfies the following criterion

$$H(\rho; \theta) > H_H = H(\rho \simeq \nu; \theta = \pi) \tag{27}$$

(which strictly applies when $\nu \gg 1$ and $(\nu - \perp\nu) \ll 1$). Under these conditions the ion can be accelerated from arbitrarily low initial velocities from the regular motion region of phase space to the stochastic region where substantial energization can occur. It is important to note that this criterion is in terms of the (initial) **Hamiltonian** and not just the (initial) **velocity** (ρ_0).

This criterion defines the allowed acceleration domain and since, unlike the single-wave criterion in Eq. (10), it does not generally coincide with the boundary between the regular and stochastic region of phase space, these two regions become connected allowing an ion to accelerate regularly (i.e. coherently) from arbitrarily low velocity and be further energized more vigorously through a stochastic interaction with the waves.

The above criterion, along with the necessary (wave-beating) condition stated in Eq. (11), represent two necessary and sufficient conditions for the beating-wave ion acceleration mechanism to occur.

Finally, it is important to mention that the criterion's independence of the wave energy ϵ is a consequence of the second-order nature of the analysis. In light of the albeit weak dependence on ϵ in the single-wave criterion in Eq. (10), we investigated numerically the dependence of the location of the critical points on the energy and found that the same dependence on ϵ applies. Therefore we can rewrite the criterion in Eq. (27) as

$$H(\rho;\theta) > H_H = H(\rho \simeq \nu - \sqrt{\epsilon}; \theta = \pi). \qquad (28)$$

A number of issues remain to be explored including: 1) the explicit form of the function ψ in Eq. (25) (which will allow us to relax the assumption $\nu - \perp\nu) \ll 1$; 2) the effects of wave dispersion and oblique propagation, 3) the extension to a collection of particles and the effects of particle collisions and 3) the experimental verification of the effect. These questions are the subject of ongoing and future investigations.

APPENDIX A: $S_6^{\nu_i,\nu_j}(\rho)$ TERM SIMPLIFICATION

Using Eq. (11) and substituting for $J_m(\rho)$ and $J'_m(\rho)$ with the following identities [18]

$$J_{m-1}(\rho) + J_{m+1}(\rho) = \frac{2m}{\rho} J_m(\rho),$$
$$J_{m-1}(\rho) - J_{m+1}(\rho) = J'_m(\rho), \qquad (A\text{-}1)$$

we can rewrite $S_6^{\nu_i,\nu_j}(\rho)$ as

$$\begin{aligned} S_6^{\nu_i,\nu_j}(\rho) = \frac{1}{8}\Bigg\{ & \sum \frac{J_{m+2}(\rho)J_{m+1}(\rho)}{\nu - m} \\ + & \sum \frac{J_m(\rho)J_{m+1}(\rho)}{\nu - m} - \sum \frac{J_{m-1}(\rho)J_{m+2}(\rho)}{\nu - m} \\ - & \sum \frac{J_m(\rho)J_{m-1}(\rho)}{\nu - m} + \sum \frac{J_{m-1}(\rho)J_{m-2}(\rho)}{\nu - m} \\ + & \sum \frac{J_{m+1}(\rho)J_{m-2}(\rho)}{\nu - m} - \sum \frac{J_m(\rho)J_{m-1}(\rho)}{\nu - m} \\ - & \sum \frac{J_m(\rho)J_{m+1}(\rho)}{\nu - m} \Bigg\}. \end{aligned} \qquad (A\text{-}2)$$

Now we use identity [19]

$$\sum_{m=-\infty}^{\infty} \frac{J_{m+p}(\rho)J_m(\rho)}{\nu - m} = \frac{\pi}{\sin \pi\nu} J_{p+\nu}(\rho)J_{-\nu}(\rho),$$

which is valid for $p > 0$ to simplify Eq. (A-2) to

$$\begin{aligned} S_6^{\nu_i,\nu_j}(\rho) &= \frac{\pi}{8 \sin \pi\nu}[2J_{\nu+2}(\rho)J_{-(\nu+1)}(\rho) \\ &- 2J_\nu(\rho)J_{-(\nu-1)}(\rho)], \end{aligned}$$

which, with the help of identities (A-1), may be easily shown to equal to

$$\begin{aligned} S_6^{\nu_i,\nu_j}(\rho) = \frac{\rho}{\nu}\frac{\pi}{\sin \pi\nu}[&J_{\nu+1}(\rho)J_{-(\nu+1)}(\rho) \\ &- J_{\nu-1}(\rho)J_{-(\nu-1)}(\rho)] \\ + \frac{\rho}{(\nu+1)}\frac{\pi}{\sin \pi(\nu+1)}[&J_\nu(\rho)J_{-\nu}(\rho) \\ &- J_{\nu+2}(\rho)J_{-(\nu+2)}(\rho)]. \end{aligned}$$

Chia *et al.* [13] showed that $S_1^{\nu_i}(\rho)$ can be simplified as

$$\begin{aligned} S_1^{\nu_i}(\rho) = \frac{\pi}{8 \sin \pi\nu_i}[&J_{\nu_i+1}(\rho)J_{-(\nu_i+1)}(\rho) \\ &- J_{\nu_i-1}(\rho)J_{-(\nu_i-1)}(\rho)]. \end{aligned}$$

It is then clear that

$$S_6^{\nu_i,\nu_j}(\rho) = \frac{\rho}{\nu_i} S_1^{\nu_i}(\rho) + \frac{\rho}{\nu_j} S_1^{\nu_j}(\rho). \qquad (A\text{-}3)$$

Finally, we caution that the relation (A-3) holds only for the special case of $\nu_i \neq$ integer and $\nu_j = \nu_i + 1$.

[1] A. Fukuyama, H. Momonta, R. Itatani, and T. Takizuka. *Phys. Rev. Lett*, 38:701, 1977.

[2] G.R. Smith and A.N. Kaufman. *Phys. Rev. Lett.*, 34:1613, 1975.

[3] C.F.F. Karney and A. Bers. *Phys. Rev. Lett*, 39:550, 1977.

[4] G.M. Zaslavsky, R.Z. Sagdeev, D.A. Usikov, and A.A. Chernikov. *Weak chaos and quasi-regular patterns*. Cambridge University Press, Cambridge, 1991.

[5] C.F.F. Karney. Stochastic ion heating by a lower hybrid wave. *Phys.Fluids*, 21(9):1584, September 1978.

[6] F. Skiff, F. Anderegg, and M.Q. Tran. Stochastic particle acceleration in an electrostatic wave. *Phys. Rev. Lett.*, 58(14):1430, April 1987.

[7] D. Benisti, A.K. Ram, and A. Bers. Ion dynamics in multiple electrostatic waves in a magnetized plasma. I. Coherent acceleration. *Phys. Plasma*, 5(9):3224, September 1998.

[8] D. Benisti, A.K. Ram, and A. Bers. Ion dynamics in multiple electrostatic waves in a magnetized plasma. II. Enhancement of the acceleration. *Phys. Plasma*, 5(9):3233, September 1998.

[9] A.K. Ram, A. Bers, and D. Benisti. Ionospheric ion acceleration by multiple electrostatic waves. *J. Geophys. Res.*, 103:9431, 1998.

[10] E.Y. Choueiri and R. Spektor. Coherent ion acceleration using two electrostatic waves. Presented at the 36^{th} AIAA Joint Propulsion Conference, Huntsville, AL, July 16-20, 2000. AIAA-2000-3759.

[11] A.J. Lichtenberg and M.A. Lieberman. *Regular and Stochastic Motion*, volume 38 of *Applied Mathematical Sciences*. Springer-Verlag, New York, 1983.

[12] H. Goldstein. *Classical Mechanics*. Addison-Wesley, Cambridge, MA, 1951.

[13] Ping-Kun Chia, L. Schmitz, and R.W. Conn. Stochastic ion behavior in subharmonic and superharmonic electrostatic waves. *Phys. Plasmas*, 3(5):1545, May 1996.

[14] R. Candy and W. Rozmus. Rational resonances in a wave driven linear oscillator. *Physica D*, 52:267, 1991.

[15] R. Candy and W. Rozmus. A symplectic integration algorithm for separable hamiltonian functions. *J. Comp. Phys.*, 92:230, 1991.

[16] R. Grimshaw. *Nonlinear Ordinary Differential Equations*. Blackwell Scientific Publications, Oxford, 1990.

[17] D. Benisti, A.K. Ram, and A. Bers. Lower bound in energy for chaotic dynamics of ions. *Phys. Lett. A*, 233:209, August 1997.

[18] G.N. Watson. *A Treatise on the Theory of Bessel Functions*. Cambridge University Press, Cambridge, 2 edition, 1962.

[19] G.M. Saslavskii, R.Z. Sagdeev, D.A. Usikov, and A. A. Chernikov. Minimal chaos, stochastic webs, and structures of quasicrystal symmetry. *Usp. Fiz. Nauk*, 156(193-251):887, October 1988.